Title	Observation of exciton-phonon sideband in individual metallic single-walled carbon nanotubes
Author(s)	Zeng, H; Zhao, H; Zhang, FC; Cui, X
Citation	Physical Review Letters, 2009, v. 102 n. 13
Issued Date	2009
URL	http://hdl.handle.net/10722/59622
Rights	Physical Review Letters. Copyright © American Physical Society.

Observation of Exciton-Phonon Sideband in Individual Metallic Single-Walled Carbon Nanotubes

Hualing Zeng,[1] Hongbo Zhao,[1,2] Fu-Chun Zhang,[1,2] and Xiaodong Cui[1,3]
[1]*Department of Physics, The University of Hong Kong, Hong Kong, China*
[2]*Center of Theoretical and Computational Physics, The University of Hong Kong, Hong Kong, China*
[3]*HKU-CAS Joint Laboratory on New Materials, The University of Hong Kong, Hong Kong, China*
(Received 11 December 2008; published 2 April 2009)

Single-walled carbon nanotubes (SWCNTs) are quasi-one-dimensional systems with poor Coulomb screening and enhanced electron-phonon interaction, and are good candidates for excitons and exciton-phonon couplings in metallic state. Here we report backscattering reflection experiments on individual metallic SWCNTs. An exciton-phonon sideband separated by 0.19 eV from the first optical transition peak is observed in a metallic SWCNT of chiral index (13,10), which provides clear evidences of excitons in metallic SWCNTs. A static dielectric constant of 10 is estimated from the reflectance spectrum.

DOI: 10.1103/PhysRevLett.102.136406 PACS numbers: 71.35.−y, 73.22.−f, 78.40.−q, 81.07.De

Single-walled carbon nanotubes (SWCNTs) have been the topic of extensive research for their potentially broad applications [1] and fundamental scientific interest. SWCNTs can be either semiconducting or metallic depending on their diameters and chiral angles. One of the important and challenging issues is the possible excitons in SWCNTs. Excitons are pairs of electrons and holes bound by the attractive Coulomb interaction, and are fundamental to our understanding of optical properties of semiconductors. After a series of theoretical and experimental works, a consensus has been reached that excitons are also prominent factors in optical transitions of semiconducting SWCNTs [2–6].

Although excitons are common in semiconductors and insulators, excitons are not expected in bulk metals because of the metallic strong Coulomb screening, which prohibits the bound state of electrons and holes in three dimensional (3D) systems. SWCNTs are quasi-1D systems with poor Coulomb screening. The relaxed bounding criteria and the much weaker screening in low dimension are in favor of the existence of excitons in metallic SWCNTs, as predicted in recent theoretical studies [7,8]. Therefore, SWCNTs provide an excellent opportunity to study the possible excitons in metallic states. In metallic SWCNTs, except for the one pair of bands that touch (or nearly touch) the Fermi surface, all pairs of bands are gapped and may form exciton-continuum manifolds [9] as in semiconducting SWCNTs. Optical measurements addressing excitons in metallic SWCNTs are challenging and only very few experiments have been reported. Very recently, Wang *et al.* reported absorption spectrum of an armchair metallic SWCNT with chiral index of (21,21). From the line shape of the optical transition, they identified the signature of exciton formation [10]. On the other hand, Berciaud *et al.* reported absorption spectrum using photothermal heterodyne detection. They found no exciton-phonon sideband and suggested weak excitonic effect in metallic SWCNTs [11]. The lack of experiments on metallic SWCNTs is partially due to the fact that photoluminescence spectroscopy, which is widely used in semiconducting SWCNTs, cannot be employed in metallic systems because of their low fluorescence yield. Resonant Raman scattering is also popular, but difficult to obtain a wide-range spectrum which is usually needed to obtain the excitonic information. In contrast, Rayleigh scattering spectroscopy monitors optical properties through scattering resonant enhancement when incident photon energy resonates with optical transition, and was demonstrated as a powerful tool to study electronic structure of both semiconducting and metallic SWCNTs [12,13].

In the present Letter, we report the backscattering reflection spectrum of suspended individual metallic SWCNTs, using a technique developed basing on Rayleigh scattering spectroscopy [14]. An exciton-phonon sideband separated by 0.19 eV from the first optical transition peak is observed in a metallic SWCNT of chiral index (13,10), which provides clear evidence of excitons in metallic SWCNTs. Our semiempirical correlated calculation shows very good agreement of exciton scenario with experiment, and estimates the static dielectric constant of the SWCNT to be 10.

The reflection experiment was performed on isolated individual SWCNTs suspended over a single slit. A 20–30 μm wide 1 mm long slit on the silicon nitride capped silicon substrate was fabricated with standard microelectromechanical systems processes, including silicon nitride etching mask growing by low pressure chemical vapor deposition (LPCVD), optical lithography, reactive ion etching, and wet etching. Microscopically long isolated SWCNTs were synthesized *in situ* across the slit by CVD method. The catalyst was prepared by selectively dipping the diluted methanol solution of $FeCl_3$ on the silicon substrate, followed by reduction in furnace under an Ar-H_2 gas flow (400–50 sccm) at 900 °C for 20 min. Individual

SWCNTs were formed on the substrate in the gas mixture of Ar-H_2/ethanol at 900 °C for an hour. SWCNTs were aligned perpendicular to the slit with the aid of the directional gas flow in the CVD process, and some examples are shown in Fig. 1(a). A supercontinuum light with wavelength from 500 nm to 2 μm was generated from an optical crystal fiber pumped by a 100 mW pulsed Nd-Yag laser (pulse width $\approx$1 ns, repetition rate = 1 kHz). The incident light beam was tightly focused by a 40× achromatic objective lens to a small spot of 4 μm on the SWCNTs, the back reflected light off the SWCNTs was collected by the same lens. The reflectance spectrum was obtained after corrections were made concerning incident light profile and geometry dependent cross section. Details about the experimental setup and data processing can be found elsewhere [14].

To identify the geometric structure of the SWCNTs, we used combined technique of micro-Raman spectroscopy and Rayleigh scattering based reflectance spectroscopy [15]. Figure 1(b) shows the spectrum of the G-mode Raman scattering of a SWCNT using a 632.8-nm excitation laser. Full width at half maximum (FWHM) of the peak is 8 cm^{-1}, indicating that this SWCNT is isolated instead of among a small bundle [16]. The asymmetric line shape of the G-mode peak, which is the so-called Breit-Wigner-Fano line shape and can be better seen from the Lorentzian fitting shown in Fig. 1(b), implies that this SWCNT is metallic. The diameter of this SWCNT is estimated to be 1.58 nm, according to the empirical relation $d = \sqrt{\frac{\omega_G^+ - \omega_G^-}{C}}$, where ω_G^+ and ω_G^- are the frequencies of the high- and low-energy G-mode subpeaks in wave numbers, respectively, and $C = 79.5$ cm^{-1} is for metallic SWCNTs [17].

Figure 2 shows the Rayleigh scattering based reflectance spectrum of this SWCNT in near-infrared to visible range [15]. There is a prominent peak at around 1.54 eV, followed by a weak sideband at ~0.19 eV higher energy. The first peak is from the first optical transition (M_{11}) for metallic SWCNTs. Using Kataura plot [18], the only candidates having the specified diameter and M_{11} energy are the (13,10) and (17,5) NTs. The latter option is, however, easily excluded on the basis that its M_{11} is split by more than 0.1 eV, due to trigonal warping effect [19]. Experimental FWHM of the M_{11} peak is only about 0.1 eV, which is consistent with the (13,10) NT whose M_{11} splitting is about 0.03 eV. Thus, we identified the geometric structure of this metallic SWCNT to be (13,10).

Free electron band-to-band transition would give a broad and unstructured reflectance spectrum of the M_{11}, and would feature an asymmetric line shape with a long tail on the high energy side, reflecting the $E^{-1/2}$-like density of states for quasi-1D systems. The reflectance spectrum shown in Fig. 2, however, presents a stark contrast. It has a well-defined *single peak*, with quite *symmetric* line shape. Accordingly excitonic nature instead of free band-to-band transition is speculated.

The strong evidence to support the exciton scenario lies in the broad sideband located at 1.73 eV with a fraction of M_{11} intensity. The intensity ratio of the sideband peak to the main peak as a function of the incident light optical density (OD) is nonlinear, as shown in Fig. 2 inset. This effectively eliminates the possibility of the continuum origin of the sideband, as the intensity ratio of continuum to an exciton would be independent of the incident light OD. The approximate energy difference of 190 meV between the sideband and M_{11} is equal to the energy of a zone-center G-mode phonon which is optically allowed. Lacking any other physical processes at this energy level, it is logical to attribute this sideband to the resonance of the incident photon with the energy of the M_{11} plus a G-mode phonon. This picture could also explain Fig. 2 inset. We speculate that the nonlinear behavior is the result of light heating effect which is due to extremely low heat capacity of the suspended SWCNTs, and can strongly affect phonon

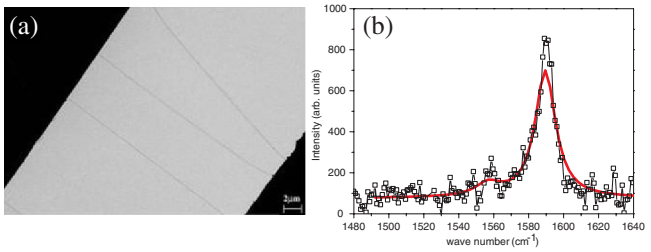

FIG. 1 (color online). (a) SEM image of three isolated carbon nanotubes suspended over the slit (white area) etched on silicon substrate (black areas at two corners). (b) *G*-mode resonant Raman spectrum of the (13,10) metallic SWCNT. Open box symbols are experimental data and the solid (red) line is a fit with two Lorentzians.

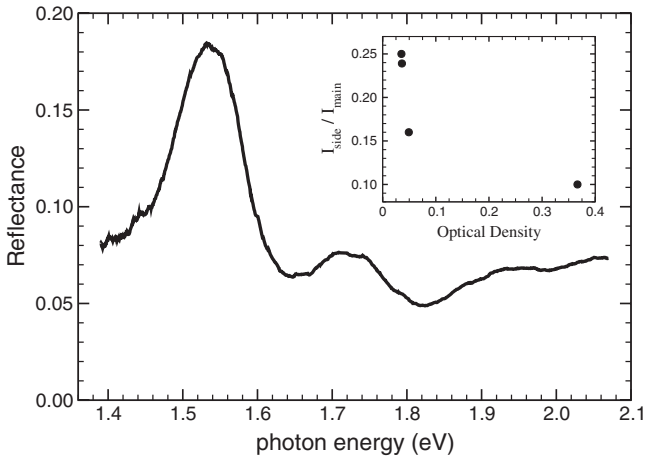

FIG. 2. Experimental reflectance spectrum of the (13,10) metallic SWCNT. Inset describes the intensity ratio of the sideband peak to the main peak as a function of the incident light optical density (OD). The average light intensity is 7×10^3 W/cm^2 at OD = 0.

population and exciton-phonon couplings [20]. Strong exciton-phonon coupling in SWCNTs has been proposed theoretically [21], and has been shown experimentally being much stronger than the coupling between free carrier and phonon [22,23]. The phonon sideband corroborates our conclusion that the main peak in reflectance arises from exciton transition in the (13,10) metallic SWCNT.

Our result supports the argument in Ref. [10]. The discrepancy with Ref. [11] may be explained by the different sample environment in the measurements. The samples here and in Ref. [10] are suspended SWCNTs in air, where the environmental dielectric constant is 1; the samples in Ref. [11] are SWCNTs isolated in surfactant micelles of SDS in D_2O, where the dielectric constants are $\sim$1.5 and 80 for SDS and D_2O, respectively, and a much stronger environmental screening is expected. We note that the exciton-phonon sideband does not show up in the absorption spectrum in Ref. [10], which could be due to weaker optical transition and shorter lifetime of the excitons associated with the M_{22} transition in their SWCNT.

To explain the experiment quantitatively, we have calculated reflectance spectrum for (13,10) metallic SWCNT using semiempirical π-electron model which can capture the low-energy physics. Electron-electron (e-e) interactions are included in the model, thus exciton physics is produced, and excellent agreements with experiments have been achieved [5,9,24,25]. The Hamiltonian is

$$H = -t\sum_{\langle ij\rangle\sigma}(c^{\dagger}_{i\sigma}c_{j\sigma} + \text{H.c.}) + U\sum_{i} n_{i\uparrow}n_{i\downarrow} + \frac{1}{2}\sum_{i\neq j} V_{ij}(n_i - 1)(n_j - 1), \quad (1)$$

where t is the nearest neighbor hopping, U is the on-site Coulomb repulsion, and V_{ij} is the long range Coulomb interaction chosen to be in the Ohno form [26]

$$V_{ij} = \frac{U}{\kappa\sqrt{1 + 0.6117R_{ij}^2}}, \quad (2)$$

where R_{ij} is distance between atoms i and j in Å, and parameter κ accounts for the dielectric screening. Taken into account that SWCNTs are similar to π-conjugated polymers [9] and that their carbon atoms are nonplanar, we chose $t = 2.0$ eV [24]. We have chosen $U = 8$ eV, same as previous calculations on semiconducting SWCNTs and π-conjugated polymers [27]. In Ref. [8], $\kappa = 3$ was selected for metallic SWCNTs, after fitting calculated M_{11} exciton energies to experimental ones for three metallic SWCNTs. The same $\kappa = 3$ was used in our calculation. Configuration Interaction of single excitations (SCI) from the Hartree-Fock (HF) ground state was used to calculate the low-energy electronic structure and dipole coupling. For (13,10) NT, we used open boundary condition and 4 unit cells, which has more than 2000 carbon atoms. In SCI calculation, 100 HF levels each from above and below Fermi surface are used, and convergence of the M_{11} energy has been reached. We have also tried Yukawa potential instead of the Ohno one, the result shows no significant difference.

From the SCI calculated electronic structure, we can get the dielectric function of an ideal macroscopic media consisting of aligned (13,10) metallic SWCNTs as [28]

$$\epsilon(\omega) = \epsilon_b - \frac{4\pi n_0}{\hbar}\sum_j \left(\frac{|d_j|^2}{\omega - E_j + i\gamma} - \frac{|d_j|^2}{\omega + E_j + i\gamma}\right). \quad (3)$$

Here, E_j and d_j are the energy and dipole coupling to the ground state, respectively, of the jth excited states obtained from the SCI calculation. Background dielectric constant ϵ_b, electron density of the media n_0, and broadening γ are the *only three* parameters we used to fit the experiment. ϵ_b should be unity if one has the complete energy spectrum. Since only the low-energy spectrum are available from the calculation, $\epsilon_b > 1$ is used to account for the effect of the missing higher energy oscillators. Reflectance can be calculated from the dielectric function using the standard formula.

In Fig. 3 the gray dots are the experimental reflectance data of the (13,10) NT. The short dashed (blue) line is the reflectance calculated from a tight binding model, with the nearest neighbor hopping being 2.85 eV to match the calculated M_{11} to the experiment. As discussed earlier, we can clearly see here the asymmetric line shape featuring a long tail on the high energy side. Tight binding calculation also produced much broader peak than the experiment. The long dashed (red) line is the fit from our SCI calculation, which has a very good agreement with the experiment for the M_{11} peak. This again shows that our

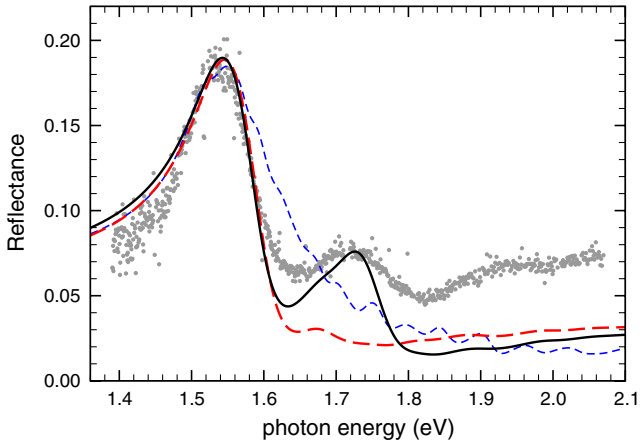

FIG. 3 (color online). Comparison of reflectance spectrum of the (13,10) metallic SWCNT between experimental data (gray dots) and different calculations (lines). The short dashed (blue) line is the reflectance calculated from a tight binding model; the long dashed (red) line is from pure SCI calculation, and the solid line is from the SCI calculation with an added phonon 0.19 eV above the first exciton.

model and calculation, which include *e*-*e* interaction, can capture the low-energy physics of SWCNTs. In the energy range shown in Fig. 3, however, reflectance from our SCI calculation shows only the M_{11} peak. Our SCI calculation does not include electron-phonon (*e*-ph) interaction, which means *e*-*e* interaction alone cannot explain the sideband, as we explain further below. The purely electronic origin of the sideband could be the splitting of the M_{11} exciton due to trigonal warping effect, or the continuum band of the exciton. The SCI calculation showed that the splitting of M_{11} is only about 20 meV, far less than the 190 meV separation. SCI calculation did give the binding energy of M_{11} exciton of (13,10) NT to be 0.2 eV, which is consistent with the poor Coulomb screening in metallic SWCNTs, and slightly smaller than the binding energy in semiconducting SWCNTs with similar diameter. However, as shown by the calculated spectrum, the continuum has very weak oscillator strength, and cannot produce a visible sideband. The only other possible origin of the sideband is then the *e*-ph interaction that was not included in our SCI calculation. With strong *e*-ph interaction, it is possible that a phonon sideband shows up in the reflectance spectrum. To test this idea, without changing any other parameters, we added a single oscillator at the energy 0.19 eV above the M_{11} exciton. The solid line in Fig. 3 shows this fitting result. Both the M_{11} and the sideband can be fitted very well. Hence, our correlated SCI calculation again showed the exciton nature of the main peak in reflectance spectrum of (13,10) metallic SWCNT.

The fitting to the reflectance spectrum produced the dielectric function, which provided an opportunity to estimate the static dielectric constant ϵ_0 of the metallic SWCNT. Dielectric constant is an important material characterization and plays an important role in the manipulation and separation of SWCNTs [29]. Theoretical calculations [30–32] and experiments have tried to establish the value, but the results vary in large range. While a fitting of the charging energy gives ϵ_0 as low as about 1.4 [33], dielectrophoresis experiments suggest it could be as high as a few hundred [29]. There is also no optical experiment to determine ϵ_0. For (13,10) NT, the best fit to the reflectance spectrum gives $\epsilon_0 \approx 10$. We note that due to difficulties in the experiment, the absolute value of reflectance intrinsically carries a relatively large error bar, which will affect the fitting result. Taking this into account, we estimated that ϵ_0 for (13,10) metallic SWCNT can be in the range of between 7 to 15.

In summary, by performing a backscattering optical reflection experiment on an isolated individual (13,10) metallic SWCNT suspended in air, we have observed a single well-defined peak in the reflectance spectrum and a pronounced exciton-phonon sideband at a higher energy of 0.19 eV in the reflectance spectrum, which clearly shows the excitonic nature of the optical transition in metallic SWCNTs. Our theoretical calculations taking into account of *e*-*e* interaction are in good agreement with the excitonic picture, and give an estimation of the static dielectric constant of $\epsilon_0 = 10$ for this SWCNT.

This work is supported by Hong Kong GRF Grants No. HKU701907P and No. HKU706707P. Computational resource from HKU's HPC Facilities is acknowledged.

[1] R. H. Baughman, A. A. Zakhidov, and W. A. de Heer, Science **297**, 787 (2002).
[2] H. Ajiki and T. Ando, J. Phys. Soc. Jpn. **62**, 1255 (1993).
[3] V. Perebeinos, J. Tersoff, and P. Avouris, Phys. Rev. Lett. **92**, 257402 (2004).
[4] C. D. Spataru *et al.*, Phys. Rev. Lett. **92**, 077402 (2004).
[5] H. Zhao and S. Mazumdar, Phys. Rev. Lett. **93**, 157402 (2004).
[6] F. Wang *et al.*, Science **308**, 838 (2005).
[7] J. Deslippe *et al.*, Nano Lett. **7**, 1626 (2007).
[8] Z. Wang *et al.*, J. Phys. Condens. Matter **21**, 095009 (2009).
[9] H. Zhao *et al.*, Phys. Rev. B **73**, 075403 (2006).
[10] F. Wang *et al.*, Phys. Rev. Lett. **99**, 227401 (2007).
[11] S. Berciaud *et al.*, Nano Lett. **7**, 1203 (2007).
[12] Z. Yu and L. Brus, J. Phys. Chem. B **105**, 1123 (2001).
[13] M. Y. Sfeir *et al.*, Science **306**, 1540 (2004).
[14] H. Zeng *et al.*, Nanotechnology **19**, 045708 (2008).
[15] Y. Wu *et al.*, Phys. Rev. Lett. **99**, 027402 (2007).
[16] A. Jorio *et al.*, Phys. Rev. B **66**, 115411 (2002).
[17] A. Jorio *et al.*, Phys. Rev. B **65**, 155412 (2002).
[18] H. Kataura *et al.*, Synth. Met. **103**, 2555 (1999).
[19] R. Saito, G. Dresselhaus, and M. S. Dresselhaus, Phys. Rev. B **61**, 2981 (2000).
[20] P. M. Ajayan *et al.*, Science **296**, 705 (2002); H. Zeng *et al.*, J. Phys. Chem. C **112**, 4172 (2008).
[21] V. Perebeinos, J. Tersoff, and P. Avouris, Phys. Rev. Lett. **94**, 027402 (2005).
[22] F. Plentz *et al.*, Phys. Rev. Lett. **95**, 247401 (2005).
[23] X. Qiu *et al.*, Nano Lett. **5**, 749 (2005).
[24] Z. Wang, H. Zhao, and S. Mazumdar, Phys. Rev. B **74**, 195406 (2006).
[25] Z. Wang, H. Zhao, and S. Mazumdar, Phys. Rev. B **76**, 115431 (2007).
[26] K. Ohno, Theor. Chim. Acta **2**, 219 (1964).
[27] M. Chandross and S. Mazumdar, Phys. Rev. B **55**, 1497 (1997).
[28] H. Haug and S. W. Koch, *Quantum Theory of the Optical and Electronic Properties of Semiconductors* (World Scientific, Singapore, 1990), 3rd ed.
[29] R. Krupke *et al.*, Science **301**, 344 (2003).
[30] L. X. Benedict, S. G. Louie, and M. L. Cohen, Phys. Rev. B **52**, 8541 (1995).
[31] M. F. Lin and D. S. Chuu, Phys. Rev. B **56**, 4996 (1997).
[32] F. Léonard and J. Tersoff, Appl. Phys. Lett. **81**, 4835 (2002).
[33] S. J. Tans *et al.*, Nature (London) **386**, 474 (1997).